Experimental evaluation of combined effect of coherent RAKE combining and SIR-based fast transmit power control for reverse link of DS-CDMA mobile radio

doi: 10.1109/49.864016

Experimental Evaluation of Combined Effect of Coherent Rake Combining and SIR-Based Fast Transmit Power Control for Reverse Link of DS-CDMA Mobile Radio

Kenichi Higuchi, Hidehiro Andoh, Koichi Okawa, Mamoru Sawahashi, *Member, IEEE*, and Fumiyuki Adachi, *Senior Member, IEEE*

***Abstract*—The combined effect of coherent Rake combining using the weighted multislot averaging (WMSA) channel estimation filter and closed-loop fast transmit power control (TPC) in the 4.096 Mchip/s direct sequence code division multiple access (DS-CDMA) mobile radio reverse link is experimentally evaluated. The WMSA channel estimation filter utilizes periodically transmitted pilot symbols (four pilot symbols are time-multiplexed in each 40-symbol time slot). Its observation period is extended to 2-K slots in order to improve the accuracy of the channel estimation. The fast TPC is based on the measurement of signal-to-interference plus background noise ratio (SIR) using pilot symbols. Laboratory experiments show that the use of the $K = 2$ WMSA channel estimation filter reduces the required E_b/I_0 at the average BER of 10^{-3} by approximately 0.5 dB compared to use of the linear interpolation filter, and that the required E_b/I_0 is minimized when the SIR measurement interval is $M = 10$ symbols (one slot TPC delay). It was also clarified that SIR-based TPC works satisfactorily when two users with different information data rates, i.e., SF, independently employ fast TPC. Field experimental results conducted in an area nearby Tokyo showed that the average BER of 10^{-3} is achieved at the target E_b/I_0 per antenna of approximately 2.5 dB by using four-finger/branch Rake and two-branch antenna diversity. Although the target E_b/I_0 to achieve same BER, when there is one interfering user with a fourfold greater transmit power than that of the desired user that independently employs fast TPC, is almost the same as that in the single-user case, the mobile transmit power is increased by 1.0–2.0 dB due to the increased MAI. These results indicate that the combination of coherent Rake combining and fast TPC works well in practical multipath fading channels.**

***Index Terms*—Adaptive transmit power control, coherent rake combining, DS-CDMA, mobile communications.**

I. Introduction

THE DIRECT sequence code division multiple access (DS-CDMA) technique has a number of advantages over TDMA and FDMA techniques, such as allowing single frequency reuse, enhancing radio transmission through Rake combining, and directly increasing capacity by using of sectored antennas [1], [2]. Based on these advantages, DS-CDMA has been widely accepted as the most promising wireless access technique. Recently, aiming at the IMT-2000 system [3], wideband DS-CDMA (W-CDMA) employing much wider spreading bandwidths than 1 MHz has been proposed [4], [5] in order to increase significantly the flexibility in offering multimedia services with different data rates. Recent developments in W-CDMA are introduced in [6]. The mobile radio channel is characterized as a multipath channel comprising many independently faded paths, each having different time delays. In the receiver, a matched filter receiver despreads and resolves the received multipath signal into multiple replicas of the narrow-band data modulated signal propagated over different paths having different delay times. These resolved signal components must be time-adjusted and coherently combined (Rake combining) to reduce the influence of multipath fading. Coherent Rake combining was adopted in both reverse and forward links in W-CDMA system. The bit-error rate (BER) performance obtainable by the use of coherent Rake combining is sensitive to the accuracy of channel estimation. It is important to develop an improved channel estimation method that works satisfactorily under slow-to-fast fading environments (for the 2-GHz carrier frequency band, the fading maximum Doppler frequency, f_D, is as high as $f_D = 185$ Hz when the traveling speed of the mobile station is 100 km/h). Thus far, several channel estimation filters have been proposed for DS-CDMA systems that periodically transmit known pilot symbols [7]–[9] (in this paper, a fine interval between the block of pilot symbols and the next block is called a time slot). Since severe multiple access interference (MAI) is produced in the asynchronous reverse link channel, closed-loop fast transmit power control (TPC) is indispensable [2]. Since DS-CDMA is, in general, an interference limited system, signal-to-average interference plus background noise ratio (SIR)-based fast TPC is the most appropriate [10], [11]. In a previous paper [12], the combined effect of coherent Rake combining and SIR-based fast TPC was experimentally evaluated; however, the channel estimation filter was a simple linear interpolation filter used pilot symbols belong to the same and the next slots. The accuracy of channel estimation improves if the channel estimation observation interval is extended to more than one slot and a larger number of pilot symbols is involved. However, in turn, the tracking

Manuscript received August 1999; revised February 28, 2000. This paper was presented in part at the First International Symposium on Wireless Personal Multimedia Communications (WPMC'98), Yokosuka, Japan, November 4–6, 1998.

K. Higuchi, H. Andoh, K. Okawa, and M. Sawahashi are with the NTT Mobile Communications Network, Inc., 3-5 Hikari-no-oka, Yokosuka-shi, Kanagawa-ken, 239-8536 Japan (e-mail: higuchi@mlab.yrp.nttdocomo.co.jp).

F. Adachi is with the Department of Electrical and Communication Engineering, Tohoku University, Miyagi 980-8579, Japan.

Publisher Item Identifier S 0733-8716(00)06119-9.

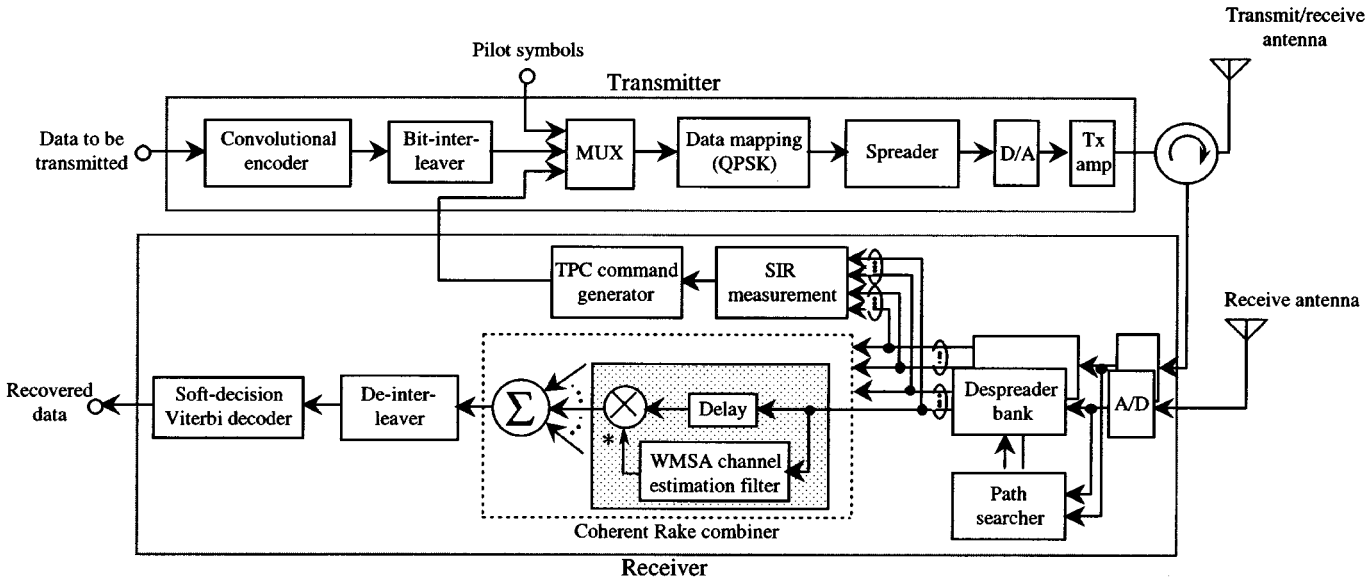

Fig. 1. Block diagram of base station W-CDMA transceiver.

ability of the channel estimation filter against fading tends to be lost. Thus, there exists a tradeoff between accuracy and the tracking ability. We proposed a pragmatic solution, i.e., the 2-K tap WMSA channel estimation filter [9], in which the observation interval is extended to 2-K slots. By setting the filter tap weights to the appropriate values, good BER performance can be achieved over a wide range of fading maximum Doppler frequencies. We also showed that the required signal energy per bit-to-interference power spectrum density (E_b/I_0) of the WMSA channel estimation filter at the average BER of 10^{-3} can be decreased by approximately 1.0 dB compared to the usage of linear interpolation filter. This results in an increase in capacity of approximately 1.3 times. Furthermore, we improved the SIR measurement method from that used in[12].

In this paper, we apply the WMSA channel estimation filter and evaluate, by both laboratory and field experiments, the combined effect of coherent Rake combining employing the WMSA channel estimation filter and SIR-based fast TPC using an implemented 4.096 Mchips/s W-CDMA transmission system. In the paper, we clarify the tradeoff relationship between the Rake time diversity effect and channel estimation accuracy in a coherent Rake receiver, and the influence of the accuracy of the SIR measurement and TPC delay on the BER performance in fast TPC. We also evaluate the BER performance in two-user environments (one interfering user) where two users using different data rate channels with different spreading factors (SF's) independently employ fast TPC. In this paper, Section II describes the experimental system and operational principles of the WMSA channel estimation filter and SIR-based fast TPC. The experimental results are discussed in Section III.

II. Experimental Configuration

A. Transmitter and Receiver Structure

The structure of the base station transceiver is shown in Fig. 1. Major radio link parameters and the frame structure of the experimental system are shown in Table I and Fig. 2, respectively, which are based on [17]. Two data rate channels were used in the experiments: 32 and 64 kb/s. The 32-kb/s (64-kb/s) data to be transmitted on the forward link (base-to-mobile) data channel were segmented into blocks of 346 (1338)-bit data (including dummy data). Each block of data plus 6 tail bits was channel-coded using convolutional coding with the rate of $R = 1/3$ and the constraint length of $K = 7$ bits (its generator polynomials are 554, 624, and 764 in octal notation). The coded data of 1056 (4032) bits were block interleaved using a 66 × 16-bit (252 × 16-bit) interleaver. After interleaving, the coded bit stream was transformed into a quaternary phase shift keyed (QPSK) symbol sequence. There were $N_p = 4$ (16) pilot symbols (modulation phase was $\pi/4$ radians) appended to every set of $N_s = 36$ (144) data symbols (including one TPC command symbol and dummy symbols) to form one slot. Each 10-ms frame comprises 16 slots of 0.625 ms each [each slot comprising $N_p + N_s = 40$ (160) symbols]. The resultant QPSK symbol rate was 64 (256) ksymbols/s $(= 1/T)$. The QPSK symbol sequence of each data

TABLE I
Radio Link Parameters

Carrier frequency (reverse/forward)		1990.5 / 2175 MHz
Chip rate (bandwidth)		4.096 Mcps (5MHz)
Symbol rate		64 ksps
Information bit rate		32 kbps
Spreading factor		64 chips/symbol
Spreading code	Scrambling code (reverse/forward)	Truncated-Gold sequence (640×2^{29} / 40960 chips)
	Short code	Orthogonal-Gold sequence (64 chips/symbol)
Modulation	Data	QPSK
	Spreading	QPSK
Channel model (laboratory tests)		L-path Rayleigh fading (equal average power)
Channel estimation		Pilot symbol-assisted WMSA channel estimation filter
Channel coding/decoding		Convolutional coding (R=1/3, k=7) / Soft-decision Viterbi decoding
Fast TPC		SIR based closed-loop

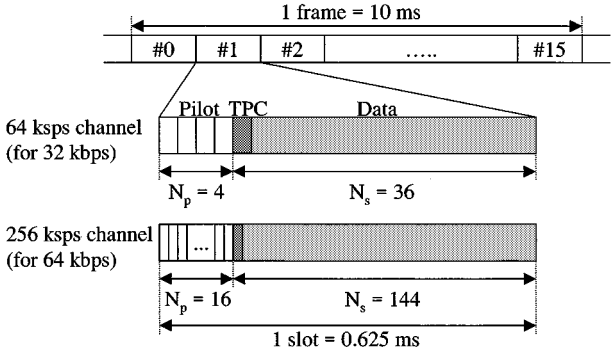

Fig. 2. Frame structure.

channel was multiplied with an orthogonal Gold sequence with the repetition period of 64 (16) chips [the spreading factor is SF $= 64$ (16)] and a scrambling code with the repetition period of 640×2^{29} chips. The orthogonal Gold sequence is generated as follows. First, a Gold sequence whose cross-correlation function has three values is generated from a pair of preferred sequences. The modulo-2 sum of the two preferred sequences produces a Gold sequence by cyclically shifting one of the pair [15]. Then, the orthogonal Gold sequence, whose cross-correlation is always zero when a zero time-shift, is generated by adding "zero" to the end of the Gold code [16]. The spreading chip rate was 4.096 Mchips/s. To confine the spread signals within the bandwidth of 5.0 MHz, a square-root raised cosine Nyquist transmit filter with the roll-off factor of 0.22 was applied before frequency conversion into the carrier frequency of 2175 MHz and power amplification. Note that the radio link parameters used in the paper are different from that of the latest standard in 3rd Generation Partnership Project (3GPP) [18] with respect to several points. In the latest 3GPP's standard, the chip rate is 3.84 Mchips/s and one frame comprises 15 slots, the length of which is 0.667 ms. The scrambling code length on the reverse link is 38 400 chips (=10 ms in time). The pilot symbols on the reverse link to be used for coherent channel estimation are multiplexed onto the quadrature (Q) channel while the coded data symbols are multiplexed onto the in-phase (I) channel. Since the difference in the slot lengths is small (0.667 versus 0.625 ms), the impact on the tracking performance of channel estimation and fast TPC against fading is considered very small. Furthermore, the impact of the difference in the pilot symbol structure (I/Q code-multiplexed against time multiplexed) on the channel estimation is also considered small because almost the same pilot power is assigned per slot. Thus, the obtained results in the paper can be applied to the latest 3 GPP's air interface.

At the reverse link (mobile-to-base) receiver, two-branch antenna diversity reception and a 4-finger/antenna Rake combiner were used. After linearly amplified by an automatic gain control (AGC) amplifier, the received spread signal at each antenna was converted into baseband in-phase (I) and quadrature phase (Q) components by a quadrature detector. The I and Q signals were sampled at a rate of 4×4.096 MHz using 8-bit A/D converters and filtered by a square-root raised cosine Nyquist filter. In a practical situation, it is very difficult to search, slot by slot, the propagation paths using the instantaneous power delay profile (measured over N_p-pilot symbol interval in each slot) because of the adverse effect of fading and severe interference. Therefore, our approach is to search the propagation paths using the block-average power delay profile. First, the instantaneous power delay profile is measured by using N_p pilot symbols belonging to each slot and, then, average them over 10 frames (=100 ms interval). While the instantaneous phase and amplitude vary within one slot due to fading, the average power delay profile shape can be assumed to remain unchanged over a 100-ms interval. From the laboratory and field experiments, the 100-ms measurement interval was found to minimize the average BER after Rake combining. The delay time resolution for the power delay profile measurement was 1/4-chip (=61.04 ns =18.31 m). Paths having a received power above a predetermined threshold, which was set to four times the minimum power in the measured power delay profile, were recorded and the four (at most) strongest were selected. The composite signal sample sequence at each antenna was despread by a matched filter (implemented by four synchronous correlators, each time synchronized to one of the four selected paths). A total of eight signals (at most) were coherently Rake combined. The soft decision data sequence from the coherent Rake combiner was deinterleaved and soft-decision Viterbi decoded to recover the transmitted data. For fast closed-loop TPC, the base station receiver measures the received SIR and generates the TPC command to raise and lower the mobile transmit power.

B. WMSA Channel Estimation Filter

Fig. 3 shows a block diagram of the WMSA channel estimation filter [9]. First, instantaneous channel estimation of the lth resolved path at the time position $t = kT_{\text{slot}} + (N_p - 1)T/2$, where $T_{\text{slot}} = (N_p + N_s)T$ (T is the symbol duration), is performed using the N_p pilot symbols belonging to the kth slot as

$$\hat{\eta}_l(k) = \frac{1}{N_p} \sum_{n=0}^{N_p-1} r_l(n, k) \tag{1}$$

where $r_l(n, k)$ is the matched filter output corresponding to the nth symbols in the kth slot for the lth resolved path. In our experiments, $N_p = 4$ (16) and $N_s = 36$ (144) for 32 kb/s (64 kb/s) data rate. Since the fading variation over the interval of N_p pilot symbols is negligible, $\hat{\eta}_l(k)$ can be approximately given by $\hat{\eta}_l(k) \approx \sqrt{2S}\xi_l(n = 0, k) + w_l(k)$, where S is the total average received signal power, $\xi_l(n = 0, k)$ is a complex-valued channel gain at $t = kT_{\text{slot}}$ of the lth path (we assume $\sum_{l=0}^{\infty} E(|\xi_l|^2) = 1$, where $E(\,)$ denotes the ensemble average), and $w_l(k)$ is a complex-valued noise component with the power of $(I_0/T)/N_p$, where I_0 is the interference plus background noise power spectrum density. The signal-to-noise ratio (SNR) of the channel estimate is N_p times larger than the received SIR per symbol. In the case of slow fading, since the channel gain remains almost the same over a period of several slots, we can extend the observation interval to more than one slot to add coherently several consecutive channel estimates. We apply a linear filter having 2-K taps. The filter output is expressed as

$$\hat{\eta}_l(k) = \sum_{i=0}^{K-1} \alpha_{-i}\hat{\eta}_l(k - i) + \sum_{i=0}^{K-1} \alpha_i \hat{\eta}_l(k + i + 1) \tag{2}$$

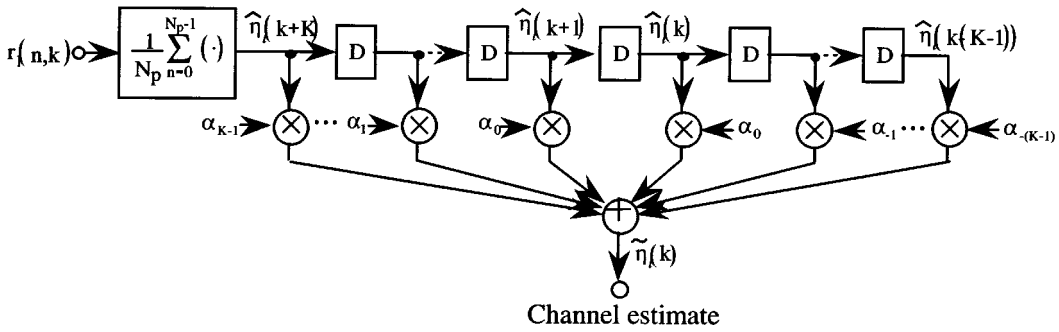

Fig. 3. WMSA channel estimation filter.

where α_i is the real-valued weighting factor (or tap coefficient). Since the magnitude of the autocorrelation function of the time-varying complex-valued channel gain is an even function with respect to the time difference, the contribution from the past and future channel gains to the channel estimate should be the same. Therefore, we set the filter coefficients, α_i and α_{-i}, equal to each other. Term $\tilde{\eta}(k)$ is used as the channel estimate at all symbol positions in the kth slot, so the channel estimate, $\tilde{\eta}(n, k)$ is represented as

$$\hat{\eta}_l(n, k) = \hat{\eta}_l(k) \qquad \text{for } n = N_p, N_p + 1, \ldots, N_p + N_s - 1. \tag{3}$$

By selecting the appropriate weighting factors, α_i's, accurate channel estimation may be possible, particularly in slow fading environments. Through computer simulations, we found the set of weighting factors for $K = 1$–3 to achieve good overall BER performance and in the following experiments, we used $\alpha_0 = 1.0$, $(\alpha_0, \alpha_1) = (1.0, 0.6)$, and $(\alpha_0, \alpha_1, \alpha_2) = (1.0, 0.8, 0.3)$ for $K = 1$, 2, and 3, respectively. On the other hand, the linear interpolation filter used as a reference is represented as

$$\hat{\eta}_l(n, k) = \left\{1 - \left(\frac{n - N_p}{N_s}\right)\right\} \hat{\eta}_l(k) + \frac{n - N_p}{N_s} \hat{\eta}_l(k+1). \tag{4}$$

Finally, Rake combiner output for data decision is represented as

$$\tilde{r}_d(n, k) = \sum_{l=0}^{L-1} r_l(n, k)\hat{\eta}_l(n, k)* \qquad \text{for } n = N_p, N_p + 1, \ldots, N_p + N_s - 1 \tag{5}$$

where L is the number of resolved paths.

C. SIR-Based TPC

In the Rake combiner, the despread signals associated with resolved paths are multiplied by the complex conjugate of their channel gain estimates and summed. Therefore, if the SIR measurement is done after Rake combining, it is affected by the channel estimation error. In this paper, instead of measuring the SIR after Rake combining, we apply the SIR measurement method proposed in [13], in which, first, the SIR on each resolved path is measured and, then, the SIR's of all the resolved paths are summed to obtain the SIR (which is equivalent to the one at the output of the Rake combiner). By doing so, an SIR measurement that has less influence on the channel estimation error is possible. Therefore, we measured the SIR associated with each resolved path and then summed them to obtain the SIR that corresponds to the SIR after Rake combining. The SIR measurement is summarized below. First, signal power $\tilde{S}_l(k)$ of the kth slot associated with the lth path is computed using the received M symbols including N_p pilot symbols. Signal power $\tilde{S}_l(k)$ is given by

$$\tilde{S}_l(k) = |\overline{r}_l(k)|^2 \tag{6}$$

where

$$\overline{r}_l(k) = \frac{1}{M}\left[\sum_{n=0}^{N_p-1} r_l(n, k)\exp\left(-\frac{j\pi}{4}\right) + \sum_{n=N_p}^{M-1} r_l(n, k)\exp\left(-j\tilde{\phi}(n, k)\right)\right] \tag{7}$$

and $\tilde{\phi}(n, k)$ is the tentative decision on the nth symbol of the kth slot. The first term in the square brackets is the contribution from N_p pilot symbols with the modulation phase of $\pi/4$ radians. Term $\tilde{\phi}(n, k)$ is given by

$$\tilde{\phi}(n, k) = \max_{\phi \in \{m\pi/2;\, m=0-3\}} \mathrm{Re}[\tilde{r}(n, k)\exp(-j\phi)] + \frac{\pi}{4} \tag{8}$$

where $\tilde{r}(n, k)$ is the Rake combiner output given by

$$\tilde{r}(n, k) = \sum_{l=0}^{L-1} r_l(n, k)\hat{\eta}_l(k)^*, \qquad 0 \le n \le M - 1 \tag{9}$$

with $\hat{\eta}_l(k)$ given by (1). Note that the above coherent Rake combining is different from that for data detection. A 2-K tap WMSA channel estimation filter used for data detection incurs a time delay of K slots. Thus, this filter cannot be used for SIR measurement because the TPC error is delay sensitive. Therefore, in order to reduce the TPC error, the channel estimation for SIR measurement is separated from that for data detection. The SIR is measured using N_p-pilot symbols only and, by doing so, the TPC delay of one slot can be achieved. The instantaneous interference plus background noise power of the lth path, $\tilde{I}_l(k)$, is computed as the squared error of the received N_p pilot samples and N_d data samples:

$$\tilde{I}_l(k) = \frac{1}{M}\sum_{n=0}^{M-1} \left| r_l(n, k)\exp\left(-j\tilde{\phi}(n, k)\right) - \overline{r}_l(k)\right|^2 \tag{10}$$

where $\tilde{\phi}(n, k) = \pi/4$ for $n = 0, 1, \ldots, N_p - 1$. Then, $\tilde{I}_l(k)$ is averaged using a first-order filter with forgetting factor $\mu(<1)$ to obtain

$$\overline{I}_l(k) = \mu \overline{I}_l(k-1) + (1-\mu)\tilde{I}_l(k). \tag{11}$$

The SIR at the kth slot associated with the lth path $\tilde{\lambda}_l(k)$ is given by

$$\tilde{\lambda}_l(k) = \tilde{S}_l(k)/\overline{I}_l(k) \tag{12}$$

and, finally, the SIR at the kth slot, $\overline{\lambda}(k)$ is obtained as

$$\overline{\lambda}(k) = \sum_{l=0}^{L-1} \tilde{\lambda}_l(k). \tag{13}$$

In the experiment, $\mu = 0.99375$ was used [i.e., the SIR measurement interval becomes $1/(1-\mu) = 160$ slots $=100$ ms] so that fast variation due to fading can be sufficiently averaged, while shadowing remains unchanged. In the following section, we used E_b/I_0 instead of $\overline{\lambda}(k)$. E_b/I_0 can be expressed using $\overline{\lambda}(k)$ as $E_b/I_0(k) = \overline{\lambda}(k) + 10\log(3/2)$ dB since rate-1/3 convolutional coding and QPSK data modulation were used. When D-branch antenna diversity is used, L should be replaced by DL. The measured $E_b/I_0(k)$ was compared to the target E_b/I_0 and the TPC command was generated, which was transmitted to raise or lower the mobile transmit power by ± 1 dB every 0.625 ms. It should be noted that the fast TPC can operate in the same way for any different data rate by computing the received E_b/I_0 from the measured SIR using the equation $\text{SIR} = 2R \cdot (E_b/I_0)$, where R is the coding rate and QPSK data modulation is assumed.

III. Experimental Results

A. Laboratory Experiments

A single-user case was evaluated since the interference from other power-controlled users can be well approximated by Gaussian noise and can be combined with the background noise. Two hardware fading simulators were used to simulate L-path ($L = 1$–4) Rayleigh fading channels for two antennas. The variances of the channel gains of $2L$ paths were assumed to be equal and $2L$ channel gains were assumed to be independent complex Gaussian processes. On the other hand, the forward link channel was not a faded channel, and its received signal power was set to be sufficiently high such that the average BER was 0. The average BER's and the averaged received E_b/I_0 (where I_0 included the multipath interference of its own channel) were measured for various values of the TPC target E_b/I_0. The measured BER's for the WMSA channel estimation filter with $K = 1, 2, 3$ and a linear interpolation filter are plotted in Fig. 4 as a function of the average E_b/I_0 per antenna for the case of $L = 2$ and $f_D = 80$ Hz in the 32-kb/s data rate channel. The TPC closed-loop delay was one time slot ($=0.625$ ms) and $M = 10$. For comparison, the computer simulation results are also plotted. Although the measured performance are degraded by about 1 dB compared to the corresponding computer simulated performance, the required E_b/I_0 at the average BER of 10^{-3} is reduced by about 0.5 dB

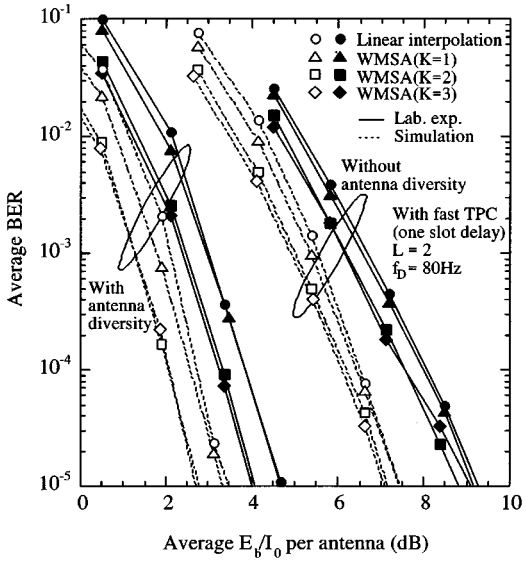

Fig. 4. Average BER as a function of average E_b/I_0 per antenna.

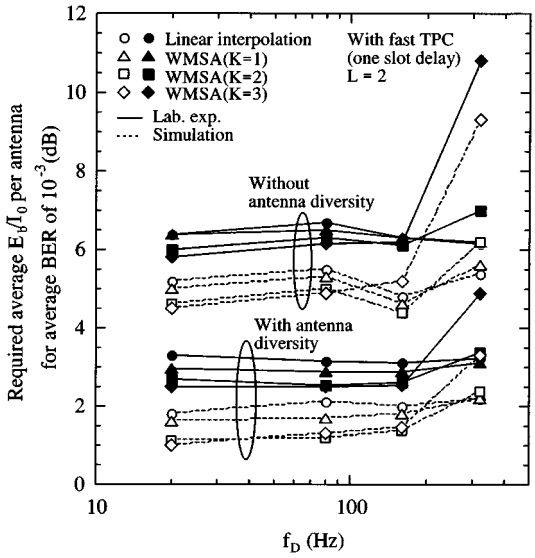

Fig. 5. Required average E_b/I_0 per antenna as a function of f_D.

using the WMSA channel estimation filter with $K = 2$ or 3, compared to the linear interpolation filter. The $K = 1$ WMSA channel estimation filter provides almost the same performance as the linear interpolation filter. Fig. 5 shows the required average E_b/I_0 for the average BER of 10^{-3} as a function of the fading maximum Doppler frequency, f_D with $L = 2$ in the 32-kb/s data rate channel. The parameters of fast TPC are the same as those in Fig. 4. The computer simulation results are also plotted as dotted lines. Fig. 5 shows that without antenna diversity reception, as f_D increases from $f_D = 20$–80 Hz, the required received E_b/I_0 slowly increases. This is because the tracking ability of the fast TPC against fading tends to be lost and, accordingly, the TPC error increases. However, as f_D increases over 80 Hz, the required E_b/I_0 starts to decrease due to the increasing effect of interleaving plus channel coding. However, as f_D increases further beyond 160 Hz, the WMSA channel estimation filter, particularly with $K = 3$, cannot track against fading and accordingly, the required E_b/I_0 increases

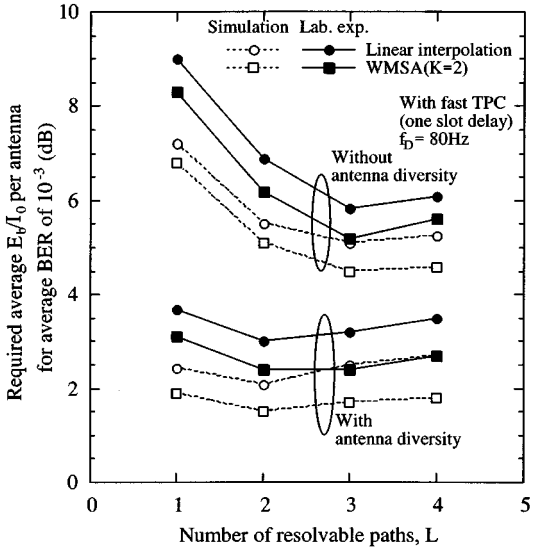

Fig. 6. Required average E_b/I_0 per antenna as a function of L.

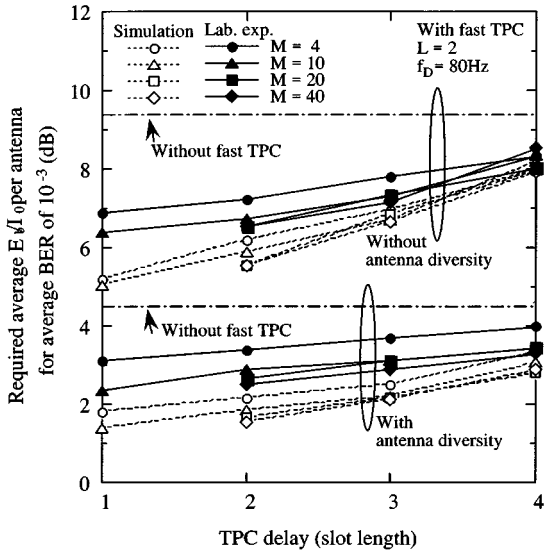

Fig. 7. Required average E_b/I_0 per antenna as a function of TPC delay with M as a parameter.

rapidly. On the other hand, when antenna diversity is applied, an almost constant required E_b/I_0 value is observed over the wide range of f_D. This is because the use of diversity reception makes the fading shallower and, thereby, reduces the TPC error but decreases the additional improvement of interleaving plus channel coding under faster fading conditions. The $K = 2$ WMSA channel estimation filter can reduce the required E_b/I_0 by about 0.5 dB for a wide range of f_D values ($<$320 Hz) compared to that of the linear interpolation filter. Furthermore, as indicated in Fig. 5, the channel estimation filters with $K = 2$ and 3 provide almost the same required E_b/I_0 when f_D is smaller than approximately 160 Hz. From Figs. 4 and 5, good overall performance can be achieved by the $K = 2$ WMSA channel estimation filter. Therefore, in the following evaluations, we used $K = 2$.

The required average E_b/I_0 at the average BER of 10^{-3} is plotted as a function of L in Fig. 6 for $f_D = 80$ Hz. Other parameters are the same as those in Fig. 4. As L increases, the required E_b/I_0 first decreases due to the increased Rake diversity effect. However, as L increases further, the received signal power per path decreases and therefore, the accuracy of the channel estimation degrades. This increases the required E_b/I_0 as L increases beyond $L = 2$. However, it should be noted that the required E_b/I_0 with antenna diversity is much smaller than without diversity, and that it is relatively insensitive to the value of L. This is explained below. When two-branch antenna diversity reception is applied, the equivalent number of resolved paths is $2L$. Therefore, the (Rake) path diversity effect can be expected even when $L = 1$. As L increases from one, the path diversity effect will increase if ideal channel estimation is assumed. However, using a practical channel estimation scheme, e.g., WMSA channel estimation, the average signal power per path decreases as L increases and, accordingly, this offsets the increasing path diversity effect. As a result, the required E_b/I_0 with antenna diversity becomes relatively insensitive to the value of L. The required E_b/I_0 is minimized at $L = 2$ and at $L = 3$ without and with antenna diversity, respectively.

SIR measurement interval M is a design parameter and is closely related to the TPC delay. In general, as M increases, the SIR measurement becomes more accurate. However, a TPC delay of more than one slot is required. As the TPC delay increases, the required E_b/I_0 increases because the ability of fast TPC to track fading degrades. Fig. 7 shows the required average E_b/I_0 for the average BER of 10^{-3} as a function of the TPC delay with M (signal power measurement interval in symbols for E_b/I_0 measurement, see Fig. 4) as a parameter in the 32-kb/s data rate channel. For comparison, the results without fast TPC are also plotted. For the given TPC delay (less than 3 slots), as M increases, the required E_b/I_0 can be reduced because accuracy of the SIR measurement improves. However, the impact of TPC delay must be considered. Using our frame structure, the TPC delay can be one slot if $M = 10$ symbols or less, but it is two slots if $M = 20$ symbols or more. As the TPC delay increases, the tracking ability of TPC against fading tends to be lost. Hence, there is a tradeoff between improved accuracy of the SIR measurement and increased TPC delay. As a result, $M = 10$ symbols (one-slot TPC delay) yields slightly lower required E_b/I_0 than $M = 40$ symbols (two-slot TPC delay). This can be seen from Fig. 7.

Based on the laboratory experimental results, we applied a $K = 2$ WMSA channel estimation filter and SIR measurement using $M = 10$ symbols in the field experiments. By applying fast TPC with SIR measurement using $M = 10$ symbols, the required E_b/I_0 was decreased by about 2.2 (3.0) dB compared to that without fast TPC with (without) antenna diversity reception for $f_D = 80$ Hz.

Until now, we assumed single-user environments, in other words, multiple access interference (MAI) was assumed as Gaussian noise. However, when the number of interfering users is small, MAI is not approximated well as Gaussian noise. Therefore, we measured the BER performance when both a 32-kb/s user with SF $= 64$ (64 ksymbols/s) and a 64-kb/s user with SF $= 16$ (256 ksymbols/s) independently employed SIR-based fast TPC. The average BER performance of the

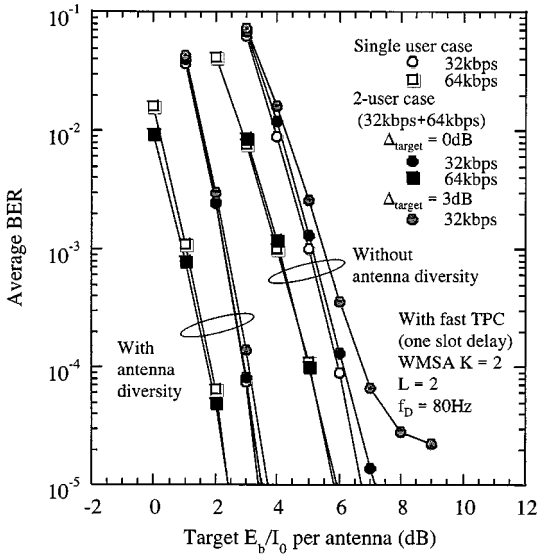

Fig. 8. Average BER as a function of target E_b/I_0 per antenna.

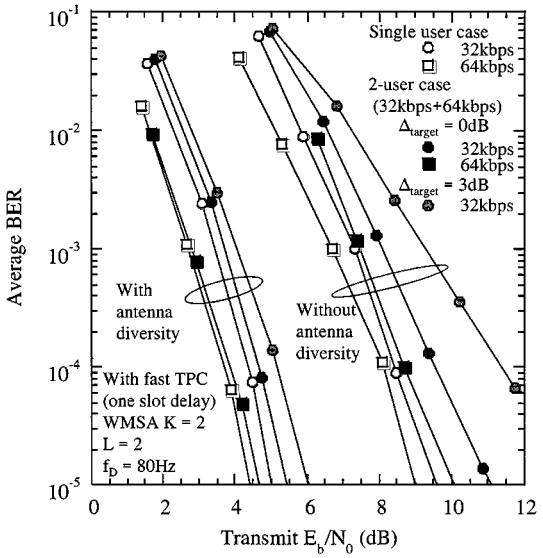

Fig. 9. Average BER as a function of average transmit E_b/N_0.

32-kb/s user and 64-kb/s user were plotted as a function of the target E_b/I_0 and the average transmit E_b/N_0 (defined as the transmit signal energy per bit-to-background noise power density ratio) at a mobile terminal in Figs. 8 and 9, respectively, assuming the same quality, i.e., same target E_b/I_0 for both users (it is denoted as $\Delta_{\rm target} = 0$ dB in the figure). The BER performance of the 32-kb/s user when target E_b/I_0 of the 64-kb/s user was $\Delta_{\rm target} = 3$ dB higher than that of the 32-kb/s user (the average transmit power of 64-kb/s user is 8 times that of the 32-kb/s user) and that when the single-user case with 32 kb/s (64 kb/s) are also plotted. One slot TPC delay and $M = 10$ (25) were assumed for the 32 (64)-kb/s data rate channel in the case of $L = 2$ and $f_D = 80$ Hz. It was observed that even when the interfering users' transmit power is four times that of the desired user, almost the same BER performance (and thus, the same required E_b/I_0) can be achieved as in the single-user case for $\Delta_{\rm target} = 0$ dB, indicating that fast TPC satisfactorily works even when an interfering user with a large transmit power exists. However, when $\Delta_{\rm target} = 3$ dB, the target E_b/I_0 of the 32-kb/s user at the average BER of 10^{-3} was increased by about 0.5 dB compared to that in the single-user case due to the fluctuation of the interference power in the SIR measurement. The target E_b/I_0 of the 64-kb/s user at the average BER of 10^{-3} is smaller by approximately 1.3 and 1.0 dB than that of the 32-kb/s user without and with antenna diversity reception, respectively. The reason for this is that the accuracy of channel estimation is better due to the increasing number of pilot symbols. On the other hand, from Fig. 9, the transmit E_b/N_0, when an interfering user exists, increases by approximately 0.4 and 0.2 dB for 32-kb/s and 64-kb/s channels, respectively, for $\Delta_{\rm target} = 0$ dB with antenna diversity reception due to the increased MAI. The transmit power of the 32-kb/s user at the average BER of 10^{-3} for $\Delta_{\rm target} = 3$ dB is increased by 0.5–1.5 dB compared to that for $\Delta_{\rm target} = 0$ dB. These figures indicate that the SIR-based fast TPC works satisfactorily for both 32-kb/s data rate channel with SF $= 64$ and the 64-kb/s data rate channel with SF $= 16$.

B. Field Experiments

The field experiments were conducted in an area near Tokyo. Measurement vehicles equipped with mobile transceivers of both desired and interfering users were driven along the measurement courses at an average speed of about 30 km/h in order to measure the BER performance in the 32 kb/s data rate channel. TPC delay was 1 slot delay and $M = 10$. The measurement courses were the same as in [12]. The right side of course #1 is a factory area, and the left side of the course is a mixture of school campuses, factories, tall apartment complexes, and houses. An elevated highway is located on the right side of course #2, and the left side of the course is a residential area. The average delay spread of the course is about 1 μs. The measured cumulative distributions of the received E_b/I_0, average BER, and mobile transmit power both for the single-user case with the 32-kb/s data rate and for the two-user case with 32-kb/s data rate (desired user) and 64-kb/s data rate (interfering user) are plotted in Fig. 10(a)–(c), respectively. For Fig. 10(a) and (b), only the performance with antenna diversity reception is shown. The target E_b/I_0 per antenna was set at 2 (5) dB with (without) antenna diversity reception to achieve almost the same BER of approximately 10^{-3} (see Fig. 11). The measured results show that even when an interfering user exits with the transmit power of four times that of the desired user, almost the same received E_b/I_0 and BER performance as the single-user case was achieved. This indicates that fast TPC worked satisfactorily when there was an interfering user with a large transmit power, while mobile transmit power at the probability of 50% increased by 1.0–2.0 dB due to the increased MAI. Fig. 10(b) and (c) clearly shows that the BER in course #2 improved, and the mobile transmit power decreased compared to that in course #1. The reason for this is that since a few paths were observed in course #2 compared to course #1, channel estimation accuracy due to increased signal power exceeded the Rake path diversity effect with antenna diversity reception (see the laboratory results in Fig. 11). The transmit power distribution can be approximated as a log normal distribution around its median value. The standard deviation is

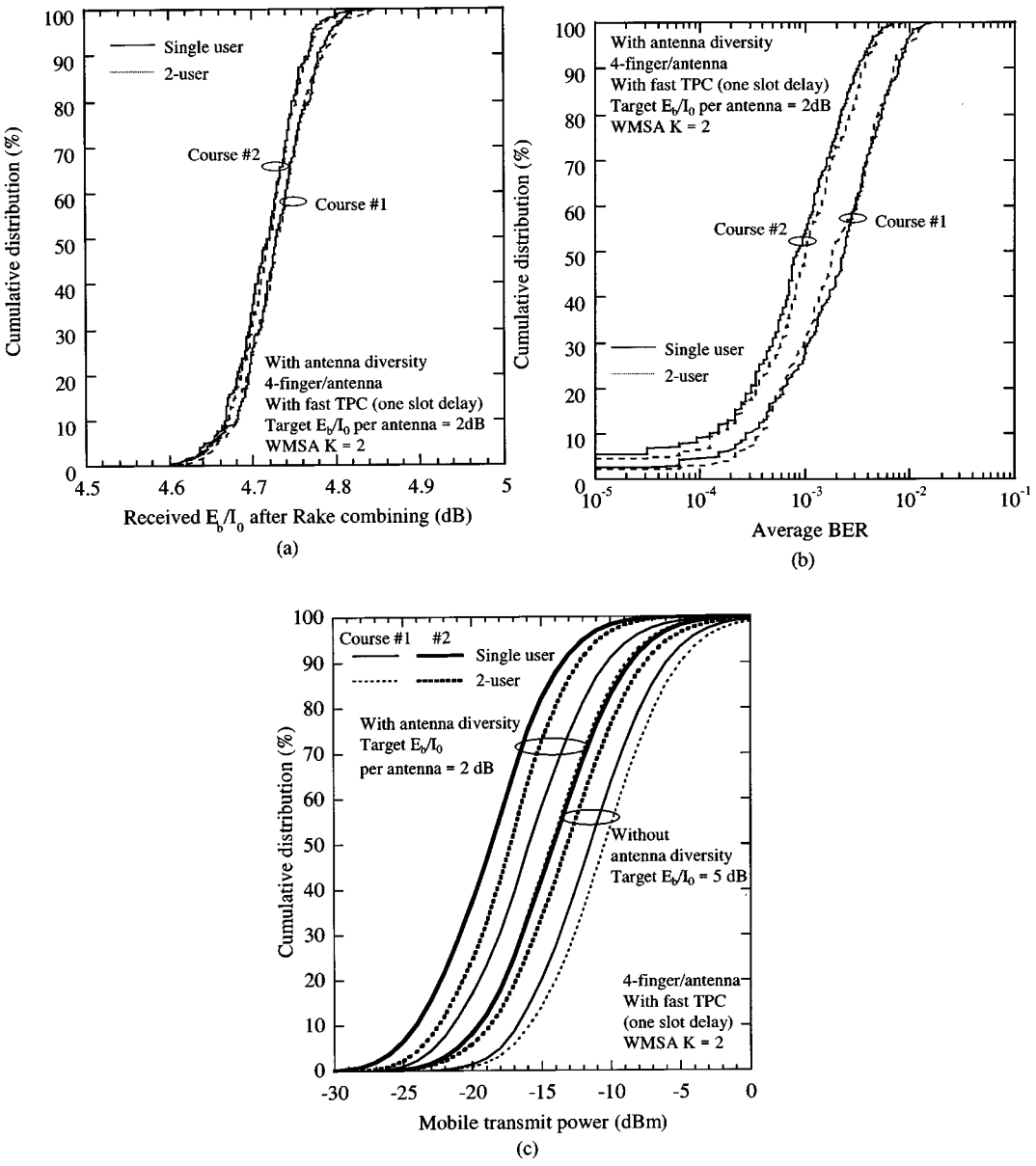

Fig. 10. Cumulative distributions of measured performance (field tests). (a) Received E_b/I_0. (b) Average BER. (c) Mobile transmit power.

about 4.44 (4.31) dB and 4.24 (4.49) dB with (without) antenna diversity for courses #1 and #2, respectively. Fig. 10(c) shows that two-branch antenna diversity reception reduces the mobile transmit power by approximately 4 dB at the median value.

Fig. 11 plots the measured average BER performance of the 32-kb/s data rate user in the single-user and two-user cases (one-interfering user with 64-kb/s data rate assuming the same BER independently employing fast TPC), as a function of the TPC target E_b/I_0 value. Laboratory experimental results of the single-user case using a uniform power delay profile with L resolvable paths are also plotted for comparison. The results clearly show that the target E_b/I_0 when the interfering user exists becomes almost the same for achieving the same BER as that of the single-user case, implying that the fast TPC worked satisfactorily in a practical fading channel. Test course #1 first experienced clear two-path and single-path fading at the middle of the course. Then, three-path fading with unequal average power was observed at the end of the course. Along course #2, two-path fading appeared first, followed by single-path fading. The measured numbers of active Rake fingers per antenna along test course #1 and course #2 are 2.0 and 1.6, respectively. Fig. 11 shows that the measured BER performance of course #1 is almost the same as the laboratory-measured BER performance when $L = 2$, and the measured BER performance of course #2 is found between the laboratory-measured BER performance when $L = 1$ and $L = 2$. The field-measured BER performance are in good agreement with those estimated from the laboratory experiment. As similarly observed by laboratory measurement, Fig. 11 shows that two-branch antenna diversity reception can reduce the target E_b/I_0 by about 3 dB at the average BER of 10^{-3}. With antenna diversity reception, the average BER of 10^{-3} can be achieved at the required E_b/I_0 of about 3 dB per antenna. Compared to the results in [12], the required target E_b/I_0 is smaller by about 2.5 dB. This

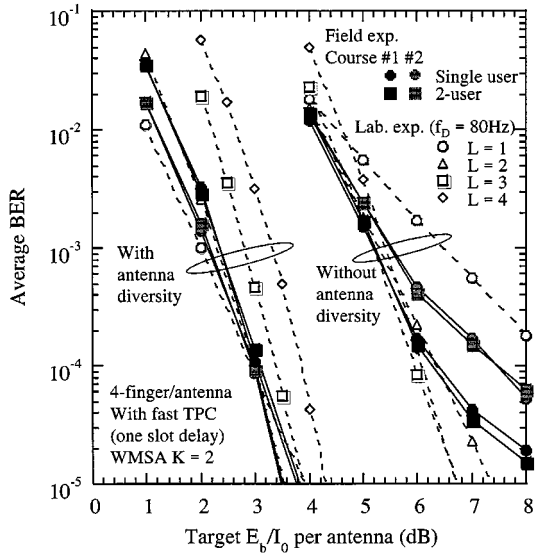

Fig. 11. Average BER as a function of average E_b/I_0 per antenna (field tests).

reduction is due to the application of the $K = 2$ WMSA channel estimation filter and the reduction of the TPC delay (in [12], a three-slot TPC delay was used).

We here calculated the long-term average mobile transmit power at the distance of 1.0 km from the cell site (on course #2) using

$$P_{TX} = L_p - (G_B + G_M - L_C) + 10\log(B) + (NF + KT) + \lambda \quad (14)$$

where $L_p(=110.7$ dB) is the path loss calculated using the Hata model [14], $G_B(=17.3$ dBi), and $G_M(=-4.7$ dBi) are the antenna gains of the base station and mobile station, respectively, which are obtained by measuring the received signal power using a receiver antenna with a dipole antenna as a reference in open space, $L_c(=5.7$ dB) is the cable loss, $B(=64$ kHz) is the data bandwidth, NF($=5$ dB) is the noise figure of the base station receiver, $KT(=-174$ dBm/Hz) is the thermal noise power spectrum density (where K is Boltzmann's constant and T is the room temperature in Kelvin degrees), and λ is the long-term average received SIR (over the measurement course #2) and is 3.0 dB at the 50% probability from Fig. 10(a). The value of the long-term average mobile transmit power calculated from (13) is -14.1 dBm. From Fig. 10(c), the median value of the measured transmit power of course #2 was -14.2 dBm, which is close to the calculated value.

IV. Conclusion

The combined effect of coherent Rake combining using the WMSA channel estimation filter and SIR-based fast TPC on the DS-CDMA reverse link was evaluated by laboratory and field experiments using the implemented 4.096 Mchips/s DS-CDMA transmission system. Laboratory experiments showed that the use of the $K = 2$ WMSA channel estimation filter reduces the required E_b/I_0 at the average BER of 10^{-3} by approximately 0.5 dB compared to use of the linear interpolation filter and that the required E_b/I_0 is minimized when SIR measurement interval $M = 10$ symbols (one slot TPC delay). We also clarified that SIR-based TPC works satisfactorily when two users with different information data rates, i.e., SF, independently employ fast TPC. Field experiments conducted in an area near Tokyo showed that the average BER of 10^{-3} is achieved at the target E_b/I_0 per antenna of approximately 2.5 dB by using four-finger/branch Rake and two-branch antenna diversity. Although the target E_b/I_0, when there is one interfering user with a fourfold greater transmit power than that of the desired user that independently employed fast TPC, is almost the same as that in the single-user case, the mobile transmit power increased by 1.0–2.0 dB due to the increased MAI. These results indicate that the combination of coherent Rake combining and fast TPC works well in practical multipath fading channels.

References

[1] A. J. Viterbi, *CDMA: Principles of Spread Spectrum Communications*. Reading, MA: Addison-Wesley, 1995.
[2] K. S. Gilhousen, I. M. Jacobs, R. Padovani, A. J. Viterbi, L. A. Weaver Jr., and C. E. Wheatly III, "On the capacity of a cellular CDMA system," *IEEE Trans. Veh. Technol.*, vol. 40, pp. 303–312, May 1991.
[3] Special Issues, IMT2000: Standards efforts of the ITU, *IEEE Personal Commun.*, vol. 4, Aug. 1997.
[4] U.-C. Fiebig, W. Granzow, W. Koch, P. Teder, and J. Thielecke, "Design study for a CDMA-based third generation mobile radio system," *IEEE J. Select. Areas Commun.*, vol. SAC-12, pp. 733–743, May 1994.
[5] F. Adachi, K. Ohno, A. Higashi, T. Dohi, and Y. Okumura, "Coherent multicode DS-CDMA mobile radio access," *IEICE Trans. Commun.*, vol. E79-B, pp. 1316–1325, Sept. 1996.
[6] Special issue, Wideband CDMA, *IEEE Commun. Mag.*, vol. 36, Sept. 1998.
[7] F. Ling, "Coherent detection with reference-symbol based estimation for direct sequence CDMA uplink communications," in *Proc. VTC'93*, NJ, May 1993, pp. 400–403.
[8] Y. Honda and K. Jamal, "Channel estimation based on time-multiplexed pilot symbols," IEICE Tech. Rep., RCS96-70, Aug. 1996.
[9] H. Andoh, M. Sawahashi, and F. Adachi, "Channel estimation filter using time-multiplexed pilot channel for coherent Rake combining in DS-CDMA mobile radio," *IEICE Trans. Commun.*, vol. E81-B, no. 7, pp. 1517–1526, July 1998.
[10] S. Ariyavisitakul, "Signal and interference statistics of a CDMA system with feedback power control—Part II," *IEEE Trans. Commun.*, vol. 42, pp. 597–605, Feb./Mar./Apr. 1994.
[11] S. Seo, T. Dohi, and F. Adachi, "SIR-based transmit power control of reverse link for coherent DS-CDMA mobile radio," *IEICE Trans. Commun.*, vol. E81-B, pp. 1508–1516, July 1998.
[12] T. Dohi, Y. Okumura, and F. Adachi, "Further results on field experiments of coherent wideband DS-CDMA mobile radio," *IEICE Trans. Commun.*, vol. E81-B, pp. 1239–1247, June 1998.
[13] Y. Amezawa and S. Sato, "A study of SIR measurement methods using signal before Rake combining," in *Rec. 1998 Spring Nat. Conv. IEICE*, Hiratsuka, Japan, March 27–30, 1998.
[14] M. Hata, "Empirical formula for propagation loss in land mobile radio service," *IEEE Trans. Veh. Technol.*, vol. VT-29, pp. 317–325, Aug. 1980.
[15] R. Gold, "Maximal recursive sequences with 3-valued recursive cross-correlation functions," *IEEE Trans. Inform. Theory*, pp. 154–156, Jan. 1968.
[16] K. Su and J. Zhu, "Performance of SSMA system by orthogonal Gold sequences," *J. China Inst. Commun.*, vol. 10, no. 2, 1989.
[17] "Specifications of air-interface for 3G mobile system Ver.0.0," Assoc. Radio Industries Businesses (ARIB), Dec. 18, 1997.
[18] 3GPP RAN 25.211 V3.1.0, Dec. 1999.

Kenichi Higuchi received the B.S. degrees from Waseda University, Tokyo, Japan, in 1994. In 1994, he joined NTT Mobile Communications Network, Inc. (now, NTT DoCoMo, Inc.). Since joining NTT Mobile Communications Network, Inc., he has been engaged in the research and development of code synchronization and interference canceller technique for wideband DS-CDMA mobile radio systems.

Hidehiro Andoh received the B.S. and M.S. degrees from Kyusyu Institute of Technology, Fukuoka, Japan. In 1993 he joined NTT Mobile Communications Network, Inc. (now, NTT DoCoMo, Inc.). Since joining NTT Mobile Communications Network, Inc., he has been engaged in the research and development of coherent RAKE receiving and interference canceller technique for wideband DS-CDMA mobile radio systems.

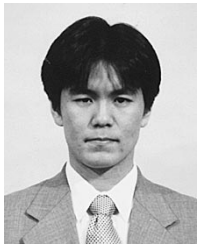

Koichi Okawa received the B.S. and M.S. degrees in electrical engineering from Keio University, Yokohama, Japan, in 1993 and 1995, respectively. In 1995, he joined NTT Mobile Communications Network, Inc. (now, NTT DoCoMo, Inc.). Since joining NTT Mobile Communications Network, Inc., he has been engaged in the research and development of radio transmission technologies for wideband DS-CDMA mobile radio systems.

Mamoru Sawahashi (M'88) received the B.S. and M.S. degrees from Tokyo University in 1983 and 1985, respectively, and received the Dr.Eng. degree from Nara Institute of Technology in 1998. In 1985 he joined NTT Electrical Communications Laboratories, and in 1992 he transferred to NTT Mobile Communications Network, Inc. (now, NTT DoCoMo, Inc.). Since joining NTT, he has been engaged in the research of modulation/demodulation techniques for mobile radio and research and development of wireless access technologies for W-CDMA mobile radio and broadband wireless packet access technologies for beyond IMT-2000. He is now the Director of the Wireless Access Laboratory of NTT DoCoMo, Inc.

Fumiyuki Adachi (M'79–SM'90) received the B.S. and Dr.Eng. degrees in electrical engineering from Tohoku University, Sendai, Japan, in 1973 and 1984, respectively.

In 1973, he joined the Electrical Communications Laboratories of Nippon Telegraph & Telephone Corporation (now, NTT) and conducted various research related to digital cellular mobile communications. From July 1992 to December 1999, he was with NTT Mobile Communications Network, Inc., where he led a research group on wideband/broadband CDMA wireless access for IMT-2000 and beyond. Since January 2000, he has been with the Graduate School of Engineering, Tohoku University, where he is a Professor of communications engineering. His research interests include: CDMA and TDMA wireless access techniques, CDMA spreading code design, Rake receiver, transmit/receive antenna diversity, adaptive antenna array, bandwidth-efficient digital modulation, and channel coding. From October 1984 to September 1985, he was a United Kingdom SERC Visiting Research Fellow in the Department of Electrical Engineering and Electronics at Liverpool University. From April 1997 to March 2000, he was a Visiting Professor at Nara Institute of Science and Technology, Japan. He has written chapters of three books: Y. Okumura and M. Shinji Eds., *Fundamentals of Mobile Communications* published in Japanese by IEICE, 1986; M. Shinji, Ed., *Mobile Communications* published in Japanese by Maruzen Publishing Co., 1989; and M. Kuwabara ed., *Digital Mobile Communications* published in Japanese by Kagaku Shinbun-sha, 1992.

Dr. Adachi was a Co-Recipient of the IEEE Vehicular Technology Transactions best paper of the year award 1980 and again 1990. He is a member of IEICE of Japan and was a co-recipient of the IEICE Transactions best paper of the year award 1996 and again 1998.